Carotid Plaque Inflammation Is Associated With Cerebral Microembolism in Patients With Recent Transient Ischemic Attack or Stroke

A Pilot Study

Ramez Reda Moustafa, MD, PhD, MRCP; David Izquierdo-Garcia, PhD; Tim D. Fryer, PhD; Martin J. Graves, PhD; James H.F. Rudd, MD, PhD, MRCP; Jonathan H. Gillard, MD, FRCR; Peter L. Weissberg, MD, FRCP, FMedSci; Jean-Claude Baron, MD, FRCP, FMedSci; Elizabeth A. Warburton, DM, MRCP

Background—Cerebral infarcts distal to carotid stenoses are thought to be caused by emboli from inflamed, destabilized plaques. We hypothesized that microembolic signals (MES) on transcranial Doppler will be associated with carotid plaque inflammation on ^{18}F fluorodeoxyglucose positron-emission tomography (FDG PET) in recently symptomatic patients.

Methods and Results—Sixteen patients presenting with recent (47±31 days) anterior circulation transient ischemic attack or minor stroke and 50% to 99% stenosis of the ipsilateral carotid bifurcation underwent FDG PET, high-resolution black-blood carotid MRI, and transcranial Doppler for detection of MES. Patients with potential cardiac sources of emboli or contralateral MES were excluded. Regions of interest defined on the coregistered MRI were used to measure FDG standardized uptake values (with Rousset partial volume correction) from the index and contralateral carotid plaques and artery. Ipsilateral MES were detected in 7 patients (MES+ group) and absent in 8 (MES− group). There was a significant difference in index-to-contralateral plaque standardized uptake value ratio between MES+ (median, 1.05; first to third quartile, 0.96 to 1.32) and MES− (median, 0.76; first to third quartile, 0.62 to 0.94) patients (P=0.005). The interval from symptom onset to PET and percent index carotid stenosis were not different between the 2 groups (P=0.68 and P=0.48, respectively).

Conclusions—In this sample of recently symptomatic patients with carotid stenosis, an association was found between in vivo measures of plaque inflammation detected by FDG PET and the presence of transcranial Doppler MES. These findings strengthen the notion that embolic events distal to carotid stenoses are related to plaque inflammation, and FDG PET may be useful in the investigation of culprit carotid lesions. **(*Circ Cardiovasc Imaging*. 2010;3:536-541.)**

Key Words: atherosclerosis ■ carotid arteries ■ stroke ■ embolism ■ transcranial Doppler ultrasonography ■ PET

Inflammation is a component of all forms of atheromatous plaques[1] and plays a key role in the destabilization of vulnerable plaques, with consequent thrombosis and distal thromboembolism.[2] Studies on carotid endarterectomy samples from symptomatic patients show an association between embolic cerebral events and active plaques with a high inflammatory infiltrate[3] and, moreover, an association of large macrophage-rich areas within such plaques and microembolic signals (MES) detected on transcranial Doppler (TCD) before surgery.[4] To date, however, these relationships have not been measured in vivo.

We and others have shown that ^{18}F fluorodeoxyglucose positron-emission tomography (FDG PET) can be used reproducibly[5–7] for noninvasive detection of atherosclerotic inflammatory activity,[6,8–10] specifically of plaque macrophages. In the present study, it was hypothesized that higher in vivo carotid plaque inflammatory activity reflected by FDG PET is associated with TCD MES in patients with carotid disease with recent transient ischemic attack (TIA) and minor stroke.

Methods

Patients

All patients recruited were aged >40 years, symptomatic within the preceding 3 months with amaurosis fugax, hemispheric TIA, or minor stroke clinically localized to the carotid territory. Patients had ipsilateral internal carotid artery stenosis of >50% by North Amer-

Received January 13, 2010; accepted June 14, 2010.

From the Department of Clinical Neurosciences (R.R.M., J.-C.B., E.A.W.), Wolfson Brain Imaging Centre (D.I.-G., T.D.F.), Department of Radiology (M.J.G., J.H.G.), and Division of Cardiovascular Medicine (J.H.F.R., P.L.W.), University of Cambridge, Cambridge, UK; and Department of Neurology (R.R.M.), Ain Shams University, Cairo, Egypt.

Correspondence to Ramez Reda Moustafa, MD, PhD, MRCP, R3 Clinical Neurosciences, Box 83, Addenbrooke's Hospital, Cambridge CB2 2QQ, UK. E-mail ramezm@msn.com

Circ Cardiovasc Imaging **is available at http://circimaging.ahajournals.org** **DOI: 10.1161/CIRCIMAGING.110.938225**

ican Symptomatic Carotid Endarterectomy Trial criteria on carotid duplex ultrasonography. The percent stenosis was determined as the median of the range provided by ultrasonography. Patients were excluded if they were claustrophobic or had other contraindications to MRI, were on anticoagulants (although single antiplatelet therapy was not a cause of exclusion because it does not significantly reduce the incidence of MES), had an inadequate temporal bone window for TCD, had a concomitant potential cardiac source of embolism established clinically or on routine investigations (eg, atrial fibrillation, recent myocardial infarction), were women of childbearing age, or had a history of major brain insult or stroke.

TCD Ultrasonography

MES in the middle cerebral arteries were detected using a pulsed Doppler device (DWL Doppler box/DWL multidop X4, 2 MHz probe) equipped with software for microemboli detection for 1 hour at 2 different insonation depths on the same day as PET. When feasible, the TCD recording was repeated on separate days to take into account the temporal variability of MES.[11,12] The recordings were witnessed, and all events and potential sources of artifacts were noted. Moreover, recordings were saved on disk for retrospective evaluation. The identification of MES was done in agreement with international recommendations[13,14] and performed both on and off line. Accepted MES were unidirectional from the baseline, lasted <0.3 seconds, and had an intensity at least 7 dB higher than that of the background flow signal. In addition, MES were associated with a characteristic chirping sound on the audible output. A finding of MES in both middle cerebral arteries during the same recording session was considered reason for secondary exclusion of patients because it suggested a noncarotid source.

PET

Imaging of the carotid arteries was done on a General Electric PET scanner using dynamic scanning in 3D mode for 75 minutes (10×5 seconds, 7×10 seconds, 4×15 seconds, 6×20 seconds, 10×30 seconds, 5×1 minute, 5×2 minutes, 10×5 minutes) immediately following injection of 185 MBq of FDG (injected over 30 seconds). A transmission scan (15 minutes) was acquired immediately before the neck FDG scan using rotating germanium-68 rod sources to allow measured attenuation correction. All images were reconstructed using the Patient-Reported Outcomes Measurement Information System 3D filtered back-projection algorithm,[15] with corrections applied for attenuation, isotope decay, dead time, normalization, scatter, sensitivity, and random coincidences (128×128×35 array; voxel size, 2.34×2.34×4.25 mm).

MRI

Scanning of the neck was done on a 1.5-T Signa Excite system equipped with a custom-designed 4-channel phased-array surface coil wrapped around the neck and secured by a soft cervical collar. Axial 2D time-of-flight magnetic resonance angiography was performed to identify the location of the carotid bifurcation and site of stenosis and was used to plan axial plaque imaging through the common carotid artery, bifurcation, and internal carotid artery and external carotid artery at least one slice above and below the identified site of stenosis. The following 2D, ECG-gated, blood-suppressed, fast spin echo pulse sequences were used for high-resolution MRI of the carotid plaques: intermediate T2W (repetition time, 2×R-R wave interval; effective echo time, 38.5 milliseconds [ms]; echo train length, 24), short T1 inversion-recovery (repetition time, 2×R-R wave interval; effective echo time, 38.5 ms; TI, 150; echo train length, 24), and T1W with fat saturation (repetition time, 1×R-R wave interval; effective echo time, 7.7 ms; echo train length, 12). The transaxial field of view was 10 cm, with a matrix size of 256×256, resulting in a voxel size of 0.39×0.39×3 mm for all 3 sequences.

To facilitate coregistration of PET to high-resolution MRI, 3D fast imaging employing steady-state acquisition sequence (repetition time, 2.5; fast response echo time, 0.9 ms; field of view, 192×192 mm; matrix, 128×128; 256 slices; slice thickness, 1.5 mm; number of excitations, 2) was used to acquire a wide-coverage image extending from the base of the skull to the midthorax without moving the patient, using the MRI system's built-in body coil.

Image Coregistration

The fast imaging employing steady-state acquisition MRIs were automatically coregistered with the high-resolution MRI using the normalized mutual information algorithm implemented in the Visualization Toolkit Computational Imaging Science Group Registration Toolkit. For each PET scan, a mean PET image was coregistered (rigid transformation) to the fast imaging employing steady-state acquisition MRI with the Max-Planck-Institute Tool software package using anatomic landmarks present on both scans, such as spinal cord, submandibular glands, and mandible. Based on the position of the artery lumens in the high-resolution MRI and the coregistered PET images, the coregistration accuracy in the region around the carotid artery was found to be ≈1.2 mm.

Image Analysis

We used a standardized uptake value (SUV) to obtain a quantitative measure of FDG uptake because it is the most widely used measure in the literature,[7,16,17] it has been shown to correlate well with more-specific quantitative measures of the FDG accumulation influx rate (K_i), and it is highly reproducible in the carotid arteries.[5]

Regions of interest were defined on the high-resolution MRI for the carotid artery ipsilateral to the symptomatic hemisphere (index carotid) and the contralateral carotid artery and transferred onto the coregistered mean PET images (last 4 frames). To correct for partial volume effects, regions of interest also were defined around all anatomic structures within a 20-mm radius (3×full width at half maximum of the scanner resolution) of each carotid artery (Figure 1), and using in-house implementation of the geometric transfer matrix MR-based method, first described by Rousset et al,[18] mean partial volume-corrected SUV was calculated. An index-to-contralateral carotid plaque partial volume-corrected SUV ratio (ICR) was calculated for each patient and used in the analyses to address inflammation in the index carotid relative to a comparable arterial site (see Discussion section). Additionally, a plaque-to-jugular venous blood SUV ratio was calculated.

Statistical Analysis

Analysis was done with SPSS version 15 for Windows. The Mann–Whitney *U* test (independent samples) or the Wilcoxon signed-rank test (paired samples) was used to compare continuous variables, including ICR, between patient groups. Values are reported as median and first to third quartile. A $P<0.05$ was considered statistically significant for all tests.

Results

General Characteristics

Sixteen patients were recruited and completed the study protocol (Table). The age of the patients was 70.5 years (57.5 to 74.8 years). Fourteen (87.5%) patients were men, 12 (75%) had hypertension, 1 was diabetic (but was normoglycemic at time of scan), 9 (56%) had a history of hypercholesterolemia, 1 had a history of ischemic heart disease, and 10 (63%) were smokers or ex-smokers.

The degree of lumen stenosis on duplex ultrasonography in the index carotid artery and the contralateral carotid artery was 69.8% (50% to 87.5%) and 0% (0% to 15%), respectively ($P<0.001$). The time interval between onset of symptoms and PET scanning was 46 days (15.8 to 80.5 days). Eleven patients eventually had carotid endarterectomy (n=9) or carotid stenting (n=2) after completing the study. The remaining patients were maintained on medical treatment. Fourteen (88%) patients were on statins at the time of PET scanning.

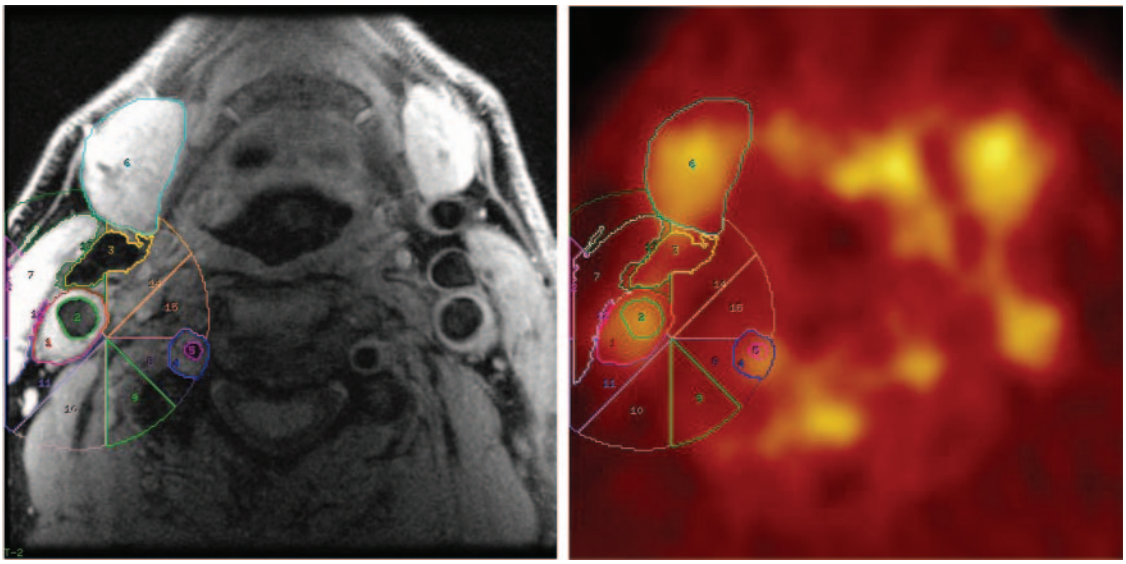

Figure 1. Regions of interest drawn around the right carotid artery used in correction for partial volume effect. 1 indicates carotid plaque/wall; 2, carotid lumen; 3, jugular lumen; 4, vertebral plaque/wall; 5, vertebral lumen; 6, submandibular gland; 7, muscle; 8 to 15, background.

FDG ICR and TCD MES

Results of TCD are shown in Table. In 1 patient, the TCD recording quality was poor because of motion and coughing artifact, so the data from this patient were not used. MES were detected on TCD in the middle cerebral artery corresponding to the index carotid artery in 7 patients (MES+ group) and were absent in 8 (MES− group). The ICR was significantly higher in MES+ patients (1.05; 0.96 to 1.32) than in MES− patients (0.76; 0.62 to 0.94; $P=0.005$) (Figures 2 and 3). Plaque-to-blood SUV ratio was also higher

Table. Summary of Clinical Characteristics and FDG PET Measurements for All the Study Patients

ID	Sex	Age	Clinical Presentation	% Stenosis*	Medications at Time of Scans†	TCD MES	Onset to PET	Index SUVmax	ICR
1	M	57	L amaurosis fugax	L ICA, 70%–80%; R ICA, 60%–70%	Clopidogrel 75 mg, simvastatin 40 mg	Yes	3 wk	4.29	1.14
2	M	72	L hemispheric TIA	L ICA, 50%–60%	Aspirin 75, simvastatin 40 mg, telmisartan 40 mg	Yes	8 wk	3.36	1.05
3	M	74	R hemispheric Stroke	R ICA, 50%; L ICA, <30%	Aspirin 75 mg, simvastatin 20 mg	Yes	10 wk	4.77	1.05
4	M	82	R hemispheric TIA	R ICA, 90%; minor plaque in L ICA	Aspirin 75 mg, clopidogrel 75 mg, simvastatin 40 mg	Yes	1 wk	2.62	0.84
5	M	56	L hemispheric TIA	L ICA, 95%; R ICA 50%–60%	Aspirin 75 mg, simvastatin 40 mg, lisinopril 5 mg, metformin 1500 mg	Yes	10 wk	3.38	1.32
6	M	75	L hemispheric TIA	L ICA, 50%	Aspirin 75 mg	Yes	5 wk	3.09	3.10
7	M	54	L hemispheric TIA	L ICA, 50 %	Aspirin 75 mg, lisinopril 10 mg, atorvastatin 40 mg	Yes	8 wk	2.59	0.96
8	F	63	R hemispheric Stroke	R ICA, 60%–69%	Aspirin 75 mg, simvastatin 40 mg	N/A	11 wk	3.68	1.38
9	M	71	L amaurosis fugax	L ICA, 80%–85%; R ICA, 70%–75%	Aspirin 75 mg, atorvastatin 20 mg, eprosartan 300 mg	No	10 wk	3.44	1.01
10	M	70	L hemispheric Stroke	L ICA, 70%–90%	Aspirin 75 mg, simvastatin 40 mg, olmisartan 10 mg	No	4 wk	4.76	0.83
11	M	70	L amaurosis fugax	L ICA, 80%–95%; minor plaque in R carotid bulb	Aspirin 75 mg	No	11 wk	6.04	0.72
12	M	59	R amaurosis fugax	R ICA, 50%	Aspirin 75 mg, atorvastatin 10 mg	No	12 wk	2.22	0.98
13	M	77	R amaurosis fugax & R hemispheric TIA	R ICA, 90%–99%	Aspirin 75 mg, simvastatin 20 mg, atenolol 100 mg	No	2 d	3.36	0.47
14	M	73	L hemispheric stroke	L ICA, 50%–70%	Aspirin 75 mg, clopidogrel 75 mg, simvastatin 40 mg	No	2 wk	3.55	0.63
15	M	76	L hemispheric stroke	L ICA, 50%	Aspirin 75 mg, simvastatin 40 mg	No	4 wk	3.85	0.62
16	F	54	L hemispheric stroke	L ICA, 80%–95%; minor plaque in R ICA	Aspirin 75 mg, simvastatin 40 mg, valsartan 160 mg, lercanidipine 10 mg	No	1 wk	4.56	0.79

ICA indicates internal carotid artery; IHD, ischemic heart disease; IBS, irritable bowel syndrome; L, left; LL, lower limb; R, right; UL, upper limb.
*On carotid duplex ultrasonography.
†Doses are per day.

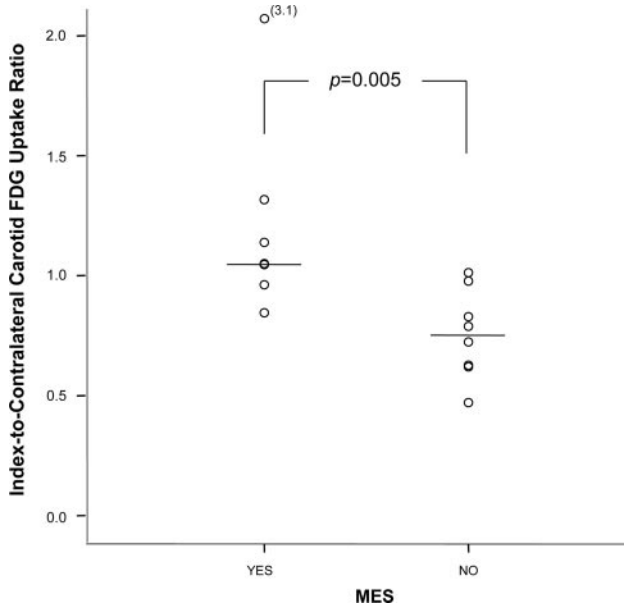

Figure 2. Dot plot of the FDG SUV ratio (index-to-contralateral carotid artery plaque) in patients with and without MES on TCD. Lines represent the median. The *P* value is for Mann–Whitney *U* test.

in the MES+ group (1.20; 0.90 to 1.70) than in the MES− group (0.96; 0.58 to 1.16), but the difference did not reach statistical significance ($P=0.17$). There was no difference in the time interval from symptom onset to PET scanning in MES+ (56 days; 21 to 70 days) and MES− ((30.5 days; 9.5 to 80.5 days) patients ($P=0.68$). In addition, the percent stenosis on carotid duplex ultrasonography in the index carotid artery was not significantly different in MES+ (55%; 50% to 90%) and MES− (81.3%; 52.5% to 87.5%) patients ($P=0.48$).

Discussion

This pilot study shows, as per the hypothesis, a significant association of TCD MES with FDG PET-detected plaque inflammation in the index carotid plaque in recently symptomatic patients. MES detected by TCD have been reported in symptomatic carotid disease and are associated with an increased risk of stroke.[19–22] Many studies correlated MES to more severe degrees of carotid stenosis,[23,24] but only a few have suggested the association of MES to morphological, as opposed to biological, features of plaque instability, such as ulcerated appearance on angiography,[22,25] an echolucent appearance on ultrasonography,[26] or plaque ulceration and surface thrombus on histological examination.[27] On the other hand, several discrepant studies[4,28,29] failed to find an association between MES and macroscopic plaque characteristics, including intraplaque hemorrhage, adherent thrombus, and surface ulceration. More directly relevant to the present investigation, however, is the finding by Jander et al[4] that the presence of TCD MES was associated with larger macrophage-rich areas in carotid endarterectomy specimens surgically removed from patients with high-grade carotid stenosis. Our results, illustrating this association in vivo, are thus entirely concordant with this earlier histopathologic investigation.

Plaque inflammation underlies a myriad of morphological changes[2] in complex and often unknown ways, which may account for the variability of association of MES to morphological features. Furthermore, some of those features that may be related to microembolism, such as small platelet aggregates and fibrin clots, usually are not specifically examined in histological specimens.[29] Finally, plaque characteristics dynamically evolve over time[2,30] and so does the frequency of MES[11,20,31]; thus, the timing of surgical intervention and of detection of MES by TCD may be critical in explaining these discrepancies. In the present study, we directly evaluated plaque inflammation in vivo by FDG PET and performed TCD on the same day, hence avoiding many of these uncertainties.

Early animal studies on FDG found that FDG accumulates in iliac artery segments with high macrophage density[32] and that its uptake is highly correlated to the macrophage count in the aorta of hyperlipidemic rabbits.[33] Autoradiography experiments using ^{3}H deoxyglucose further confirmed accumulation in inflammatory cells within human carotid plaques, but

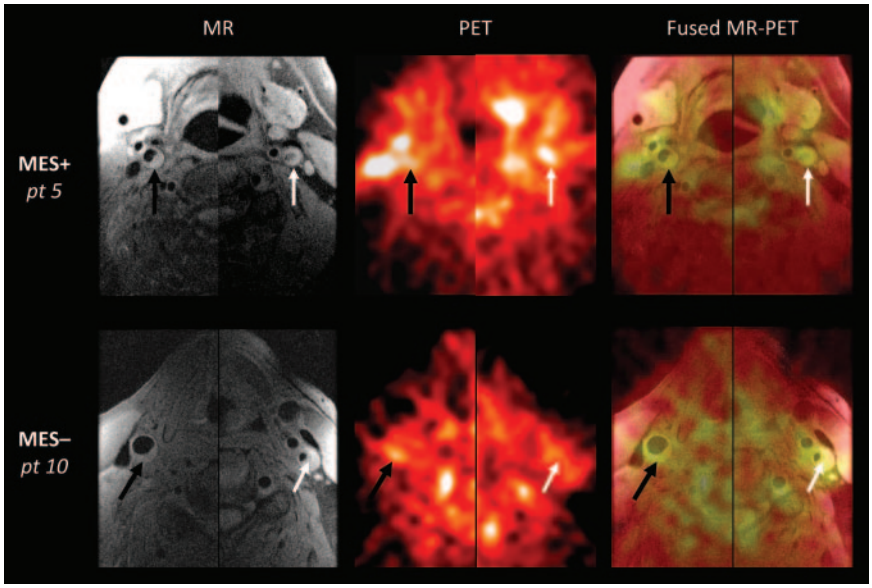

Figure 3. Axial high-resolution MRI, FDG PET, and coregistered PET-MRI of the neck in patient 5 (MES+) and in patient 10 (MES−) on TCD to illustrate the findings from the study. Note that higher FDG accumulation in the left (index) carotid plaque in the MES+ patient, whereas accumulation in the left (index) is lower than in the right (contralateral) carotid plaque in the MES− patient. For illustrative purposes, these images are composed of 2 halves, each showing the highest degree of stenosis, whereas, as explained in Methods section, the FDG uptake was quantitatively determined from the entire plaque volume.

not in the intima or smooth muscle cells.[6] Moreover, Tawakol et al[17] used in vivo FDG PET in humans to show that the ratio of carotid plaque SUV to blood-pool SUV correlated very well to macrophage staining from corresponding histological sections and noted that FDG uptake was not correlated with plaque area, plaque thickness, or area of smooth muscle cell or collagen staining. The current results showing a significant association between MES and carotid plaque FDG uptake thus suggest a relationship between MES and plaque inflammatory cell (macrophage) content.

The choice of parameters to represent inflammation in FDG PET imaging of atherosclerosis is still evolving. A ratio of plaque uptake to a background reference, such as venous blood pool[7,17] or normal-appearing arterial wall,[8] has been used in previous studies to account for interpatient variability of FDG uptake over and above the normalization to injected activity and body weight that is inherent in SUV. This plaque-to-background ratio may not be optimal because FDG uptake in atherosclerotic plaques appears to be slow[7,8] and, thus, may remain close to blood-pool activity despite long scanning times, promoting false-negative results. Furthermore, absolute SUV or tissue-to-blood ratio in a plaque may indeed represent its macrophage content,[6,17] but given that clinically silent plaques occasionally show a similar inflammatory burden to index plaques,[8,34] the direct relevance of those measures to clinical symptoms and embolism (eg, a threshold effect) is not clear. In the present study, we elected to represent index carotid plaque uptake as the ratio of partial volume-corrected SUV to that in the contralateral carotid plaque and calculated the SUV plaque-to-blood ratio for comparison. We found a consistent, though statistically borderline, result.

More importantly, the diffuse nature of arterial inflammation[34,35] suggests that inflammation measurements in a particular artery should be interpreted in the context of inflammation elsewhere in the arterial tree. Our results show that when FDG uptake was lower in the index carotid than on the contralateral side (ICR$<$1), there was no significant association with the presence of microemboli. By contrast, when FDG uptake was higher in the index carotid (ICR$\geq$1), there was a significant association between the 2 modalities. This result suggests that when index plaque inflammation is lower than the prevailing level of diffuse inflammation in comparable arterial sites, it may indicate that either the mechanism of symptoms in that case was not inflammation-driven embolism (eg, hemodynamic); that the carotid plaque was not the "culprit" lesion; or that inflammation within it has rapidly subsided, and the plaque has become quiescent in terms of embolic potential. These propositions about the dynamics of plaque inflammation cannot be confirmed in a cross-sectional study and will need to be ascertained in longitudinal prospective studies. Further, because all the contralateral plaques in this study were by design MES$-$, the relationship of microembolism to inflammation appears only true for the index carotid plaque in symptomatic patients, suggesting that inflammation interacts with other local plaque factors[2,35] to produce MES or, more generally, symptoms. A different mechanism may underlie microembolism from silent carotid plaques in asymptomatic individuals[36] and is worth investigating in future studies.

The relatively small number of patients is a limitation in the present study, and although rigorous methods were used to ensure accurate coregistration of MRI and PET data, and partial volume correction was used to reduce quantification errors in the FDG signal, the results need to be reproduced in larger samples of patients. Small samples have limited power for detection of differences between groups, yet the positive results regarding the relationships between carotid FDG uptake and the presence of microemboli in index plaques in the current sample, although not definitive, provide proof-of-principle pilot results that would justify pursuing future lines of research in this area. These relationships also will need to be compared in asymptomatic controls harboring similar degrees of carotid stenosis, as would the temporal evolution of inflammation detected by FDG PET need to be prospectively investigated.

From previous studies, it has been suggested that the macrophage content of plaques remains relatively unchanged in the first 180 days following an event.[37,38] All our patients were scanned within this time frame, yet in future studies, it would still be desirable to further shorten the interval between event onset and scanning to reduce intersubject variability. Most patients were on statins at the time of scanning in the present study, and although statins may reduce plaque inflammation,[16] clinically used doses have not been shown to have a significant effect in this time frame.

In conclusion, this study shows an association in vivo between the presence of MES on TCD and the relative intensity of plaque inflammation detected by FDG PET in carotid plaques in a sample of recently symptomatic patients with TIA and minor stroke. This finding is consistent with earlier indirect reports and if borne out in larger studies, would indicate that FDG carotid plaque imaging has direct clinical relevance to the evaluation of the risk of microembolic events.

Acknowledgments

We thank the Stroke Unit nurses and the Wolfson Brain Imaging Centre radiochemistry staff and radiographers for their assistance.

Sources of Funding

This study was funded by a Programme Grant from the British Heart Foundation (RG/03/013). Professor Weissberg is employed by the British Heart Foundation. Dr Izquierdo-Garcia is supported by the British Heart Foundation grant. This work also was supported by the Comprehensive Biomedical Research Centre grant to the Cambridge University Hospitals National Health Service Foundation Trust and Cambridge University (Cardiovascular Theme). Dr Moustafa is supported by a grant from the Cambridge Overseas Trust, United Kingdom.

Disclosures

None.

References

1. Ross R. Atherosclerosis: an inflammatory disease. *N Engl J Med*. 1999; 340:115–126.
2. Spagnoli LG, Bonanno E, Sangiorgi G, Mauriello A. Role of inflammation in atherosclerosis. *J Nucl Med*. 2007;48:1800–1815.
3. Spagnoli LG, Mauriello A, Sangiorgi G, Fratoni S, Bonanno E, Schwartz RS, Piepgras DG, Pistolese R, Ippoliti A, Holmes DR Jr. Extracranial thrombotically active carotid plaque as a risk factor for ischemic stroke. *JAMA*. 2004;292:1845–1852.

4. Jander S, Sitzer M, Schumann R, Schroeter M, Siebler M, Steinmetz H, Stoll G. Inflammation in high-grade carotid stenosis: a possible role for macrophages and T cells in plaque destabilization. *Stroke*. 1998;29:1625–1630.
5. Izquierdo-Garcia D, Davies JR, Graves MJ, Rudd JH, Gillard JH, Weissberg PL, Fryer TD, Warburton EA. Comparison of methods for magnetic resonance-guided [18-F]fluorodeoxyglucose positron emission tomography in human carotid arteries. reproducibility, partial volume correction, and correlation between methods. *Stroke*. 2009;40:86–93.
6. Rudd JH, Warburton EA, Fryer TD, Jones HA, Clark JC, Antoun N, Johnstrom P, Davenport AP, Kirkpatrick PJ, Arch BN, Pickard JD, Weissberg PL. Imaging atherosclerotic plaque inflammation with [18F]-fluorodeoxyglucose positron emission tomography. *Circulation*. 2002; 105:2708–2711.
7. Rudd JH, Myers KS, Bansilal S, Machac J, Pinto CA, Tong C, Rafique A, Hargeaves R, Farkouh M, Fuster V, Fayad ZA. Atherosclerosis inflammation imaging with 18F-FDG PET: carotid, iliac, and femoral uptake reproducibility, quantification methods, and recommendations. *J Nucl Med*. 2008;49:871–878.
8. Davies JR, Rudd JH, Fryer TD, Graves MJ, Clark JC, Kirkpatrick PJ, Gillard JH, Warburton EA, Weissberg PL. Identification of culprit lesions after transient ischemic attack by combined 18F fluorodeoxyglucose positron-emission tomography and high-resolution magnetic resonance imaging. *Stroke*. 2005;36:2642–2647.
9. Warburton L, Gillard J. Functional imaging of carotid atheromatous plaques. *J Neuroimaging*. 2006;16:293–301.
10. Tahara N, Kai H, Nakaura H, Mizoguchi M, Ishibashi M, Kaida H, Baba K, Hayabuchi N, Imaizumi T. The prevalence of inflammation in carotid atherosclerosis: analysis with fluorodeoxyglucose-positron emission tomography. *Eur Heart J*. 2007;28:2243–2248.
11. Molloy J, Khan N, Markus S. Temporal variability of asymptomatic embolization in carotid artery stenosis and optimal recording protocols. *Stroke*. 1998;29:1129–1132.
12. Droste DW, Decker W, Siemens HJ, Kaps M, Schulte-Altedorneburg G. Variability in occurrence of embolic signals in long term transcranial Doppler recordings. *Neurol Res*. 1996;18:25–30.
13. Ringelstein EB, Droste DW, Babikian VL, Evans DH, Grosset DG, Kaps M, Markus HS, Russel D, Siebler M. Consensus on microembolus detection by TCD. *Stroke*. 1998;29:725–729.
14. Symposium CCotNICH. Basic identification criteria of Doppler microembolic signals. *Stroke*. 1995;26:1123.
15. Kinahan PE, Rogers JG. Analytical 3D image reconstruction using all detected events. *IEEE Trans Nucl Sci*. 1989;36:964–968.
16. Tahara N, Kai H, Ishibashi M, Nakaura H, Kaida H, Baba K, Hayabuchi N, Imaizumi T. Simvastatin attenuates plaque inflammation: evaluation by fluorodeoxyglucose positron emission tomography. *J Am Coll Cardiol*. 2006;48:1825–1831.
17. Tawakol A, Migrino RQ, Bashian GG, Bedri S, Vermylen D, Cury RC, Yates D, LaMuraglia GM, Furie K, Houser S, Gewirtz H, Muller JE, Brady TJ, Fischman AJ. In vivo 18F-fluorodeoxyglucose positron emission tomography imaging provides a noninvasive measure of carotid plaque inflammation in patients. *J Am Coll Cardiol*. 2006;48:1818–1824.
18. Rousset OG, Ma Y, Evans AC. Correction for partial volume effects in PET: principle and validation. *J Nucl Med*. 1998;39:904–911.
19. Valton L, Larrue V, le Traon AP, Massabuau P, Geraud G. Microembolic signals and risk of early recurrence in patients with stroke or transient ischemic attack. *Stroke*. 1998;29:2125–2128.
20. Siebler M, Kleinschmidt A, Sitzer M, Steinmetz H, Freund HJ. Cerebral microembolism in symptomatic and asymptomatic high-grade internal carotid artery stenosis. *Neurology*. 1994;44:615–618.
21. Hennerici M. High-intensity transient signals: evolution or revolution in understanding cerebral embolism? *Eur Neurol*. 1995;35:249–253.
22. Valton L, Larrue V, Arrue P, Geraud G, Bes A. Asymptomatic cerebral embolic signals in patients with carotid stenosis. Correlation with appearance of plaque ulceration on angiography. *Stroke*. 1995;26:813–815.
23. Molloy J, Markus HS. Asymptomatic embolization predicts stroke and TIA risk in patients with carotid artery stenosis. *Stroke*. 1999;30: 1440–1443.
24. Siebler M, Nachtmann A, Sitzer M, Rose G, Kleinschmidt A, Rademacher J, Steinmetz H. Cerebral microembolism and the risk of ischemia in asymptomatic high-grade internal carotid artery stenosis. *Stroke*. 1995;26:2184–2186.
25. Orlandi G, Parenti G, Bertolucci A, Puglioli M, Collavoli P, Murri L. Carotid plaque features on angiography and asymptomatic cerebral microembolism. *Acta Neurol Scand*. 1997;96:183–186.
26. Mayor I, Comelli M, Vassileva E, Burkhard P, Sztajzel R. Microembolic signals and carotid plaque morphology: a study of 71 patients with moderate or high grade carotid stenosis. *Acta Neurol Scand*. 2003;108:114–117.
27. Sitzer M, Muller W, Siebler M, Hort W, Kniemeyer HW, Jancke L, Steinmetz H. Plaque ulceration and lumen thrombus are the main sources of cerebral microemboli in high-grade internal carotid artery stenosis. *Stroke*. 1995;26:1231–1233.
28. Zuromskis T, Wetterholm R, Lindqvist JF, Svedlund S, Sixt C, Jatuzis D, Obelieniene D, Caidahl K, Volkmann R. Prevalence of micro-emboli in symptomatic high grade carotid artery disease: a transcranial Doppler study. *Eur J Vasc Endovasc Surg*. 2008;35:534–540.
29. Stork JL, Kimura K, Levi CR, Chambers BR, Abbott AL, Donnan GA. Source of microembolic signals in patients with high-grade carotid stenosis. *Stroke*. 2002;33:2014–2018.
30. Corti R, Hutter R, Badimon JJ, Fuster V. Evolving concepts in the triad of atherosclerosis, inflammation and thrombosis. *J Thromb Thrombolysis*. 2004;17:35–44.
31. Forteza AM, Babikian VL, Hyde C, Winter M, Pochay V. Effect of time and cerebrovascular symptoms of the prevalence of microembolic signals in patients with cervical carotid stenosis. *Stroke*. 1996;27:687–690.
32. Lederman RJ, Raylman RR, Fisher SJ, Kison PV, San H, Nabel EG, Wahl RL. Detection of atherosclerosis using a novel positron-sensitive probe and 18-fluorodeoxyglucose (FDG). *Nucl Med Commun*. 2001;22:747–753.
33. Ogawa M, Ishino S, Mukai T, Asano D, Teramoto N, Watabe H, Kudomi N, Shiomi M, Magata Y, Iida H, Saji H. (18)F-FDG accumulation in atherosclerotic plaques: immunohistochemical and PET imaging study. *J Nucl Med*. 2004;45:1245–1250.
34. Tang T, Howarth SP, Miller SR, Trivedi R, Graves MJ, King-Im JU, Li ZY, Brown AP, Kirkpatrick PJ, Gaunt ME, Gillard JH. Assessment of inflammatory burden contralateral to the symptomatic carotid stenosis using high-resolution ultrasmall, superparamagnetic iron oxide-enhanced MRI. *Stroke*. 2006;37:2266–2270.
35. Lutgens E, van Suylen RJ, Faber BC, Gijbels MJ, Eurlings PM, Bijnens AP, Cleutjens KB, Heeneman S, Daemen MJ. Atherosclerotic plaque rupture: local or systemic process? *Arterioscler Thromb Vasc Biol*. 2003; 23:2123–2130.
36. Ritter MA, Jurk K, Schriek C, Nabavi DG, Droste DW, Kehrel BE, Bernd Ringelstein E. Microembolic signals on transcranial Doppler ultrasound are correlated with platelet activation markers, but not with platelet-leukocyte associates: a study in patients with acute stroke and in patients with asymptomatic carotid stenosis. *Neurol Res*. 2009;31:11–16.
37. Peeters W, Hellings WE, de Kleijn DP, de Vries JP, Moll FL, Vink A, Pasterkamp G. Carotid atherosclerotic plaques stabilize after stroke: insights into the natural process of atherosclerotic plaque stabilization. *Arterioscler Thromb Vasc Biol*. 2009;29:128–133.
38. Redgrave JN, Lovett JK, Gallagher PJ, Rothwell PM. Histological assessment of 526 symptomatic carotid plaques in relation to the nature and timing of ischemic symptoms: the Oxford plaque study. *Circulation*. 2006;113:2320–2328.

Circulation
Cardiovascular Imaging

Carotid Plaque Inflammation Is Associated With Cerebral Microembolism in Patients With Recent Transient Ischemic Attack or Stroke: A Pilot Study

Ramez Reda Moustafa, David Izquierdo-Garcia, Tim D. Fryer, Martin J. Graves, James H.F. Rudd, Jonathan H. Gillard, Peter L. Weissberg, Jean-Claude Baron and Elizabeth A. Warburton

Circ Cardiovasc Imaging. 2010;3:536-541; originally published online July 16, 2010;
doi: 10.1161/CIRCIMAGING.110.938225
Circulation: Cardiovascular Imaging is published by the American Heart Association, 7272 Greenville Avenue, Dallas, TX 75231

Print ISSN: 1941-9651. Online ISSN: 1942-0080